

Integrating Citizen Scientist Data into the Surveillance System for Avian Influenza Virus, Taiwan

Hong-Dar Isaac Wu, Ruey-Shing Lin, Wen-Han Hwang,
Mei-Liang Huang, Bo-Jia Chen, Tseng-Chang Yen, Day-Yu Chao

The continuing circulation and reassortment with low-pathogenicity avian influenza Gs/Gd (goose/Guangdong/1996)-like avian influenza viruses (AIVs) has caused huge economic losses and raised public health concerns over the zoonotic potential. Virologic surveillance of wild birds has been suggested as part of a global AIV surveillance system. However, underreporting and biased selection of sampling sites has rendered gaining information about the transmission and evolution of highly pathogenic AIV problematic. We explored the use of the Citizen Scientist eBird database to elucidate the dynamic distribution of wild birds in Taiwan and their potential for AIV exchange with domestic poultry. Through the 2-stage analytical framework, we associated nonignorable risk with 10 species of wild birds with ≥ 100 significant positive results. We generated a risk map, which served as the guide for highly pathogenic AIV surveillance. Our methodologic blueprint has the potential to be incorporated into the global AIV surveillance system of wild birds.

Mapping the interface risk between wild birds and poultry requires information of wild bird distribution and migration patterns. Bird band recovery or global positioning system (GPS) tracking data are used for spatial risk mapping. Recently, citizen science data has become an increasingly valuable source for addressing a wide range of ecologic research questions. With this study, we provided the analytical framework of using eBird, a Citizen Scientist database (<https://www.citizenscience.gov>), to elucidate the dynamic distribution of wild birds and their potential for avian influenza virus (AIV) exchange with

domestic poultry. We generated a risk map that can be integrated into the current AIV surveillance system, enabling strategic allocation of limited resources for spatially targeted virologic surveillance. The coding source, the open terrestrial environmental dataset, and eBird dataset are fully available at <http://aiv.nchu.edu.tw>.

AIV is an influenza A virus that belongs to the Orthomyxoviridae family. AIVs have been identified in a wide variety of species of wild and domestic birds, but their natural reservoir is wild waterbirds of the orders Anseriformes and Charadriiformes (e.g., ducks, geese, swans, and shorebirds). Wild waterbirds maintain a diverse group of low-pathogenicity avian influenza A viruses (LPAIVs), which cause limited illness in these host species (1). On the contrary, highly pathogenic influenza A viruses (HPAIVs), characterized by mortality of gallinaceous poultry, are limited to H5 or H7 subtypes and continue to cause illness and death in poultry worldwide (2,3). Periodically, human infections associated with HPAIV have been detected (4). In particular, the Eurasian (goose/Guangdong/1996 [Gs/Gd]) lineage has substantially affected global epizootic outbreaks of highly pathogenic avian influenza (HPAI), which have become enzootic in some areas and involve multiple waves of influenza with genetically distinct virus clades and subclades (5). Wild geese and ducks may form the bridge for AIV transmission between wild and domestic birds, which are kept alongside each other, creating the opportunity for genetic mixing of HPAIVs and LPAIVs when they infect the same bird concomitantly. Such genetic mixing promotes bidirectional virus exchange between wild and domestic birds for the continued adaptation of Gs/Gd HPAIVs in wild bird hosts and long-distance spread to new geographic regions along the flyway (6–8). Information about where wild and domestic birds can

Author affiliations: National Chung Hsing University, Taichung, Taiwan (H.-D.I. Wu, W.-H. Hwang, M.-L. Huang, B.-J. Chen, T.-C. Yen, D.-Y. Chao); Taiwan Endemic Species Research Institute, Jiji Town, Taiwan (R.S. Lin)

DOI: <https://doi.org/10.3201/eid2901.220659>

potentially interact on the landscape can help identify areas where disease transmission may be more likely to occur, useful for risk management and control measures. Such regions could become focal areas for surveillance and prevention (9).

The first step of mapping the interface risk requires information of wild bird distribution and migration patterns; however, obtaining such information is difficult. Without empirical data, previous studies implemented simulations or mathematical modeling for spatial risk mapping (10–13). Meanwhile, bird migration routes can be acquired from the bird band recovery (14) or GPS tracking data (15), but only a limited number of wild birds can be tracked and analyzed. Citizen science data are valuable for addressing a wide range of ecologic research questions, and the scope and volume of available data have rapidly increased globally (16). However, data from large-scale citizen science projects typically present a number of challenges that can inhibit robust ecologic inferences, including species bias, spatial bias, varied efforts, and varied observer skills (17–19). When using citizen science data, it is imperative to carefully consider the data processing and analytical procedures required to appropriately address the bias and variation.

Since 2015, Taiwan, which is on the East Asian Flyway of bird migration, has been affected by HPAI H5 virus clade 2.3.4.4, resulting in tremendous economic loss (20,21). In this study, we established an analytical framework (Figure 1) using citizen science data, eBird (22), to map the interface risk between wild birds and poultry flocks and to shed light on the underlying mechanism of AIV transmission in

Taiwan. Our risk map presents a quantitative evaluation of the risk for AIV exchange at the interface between poultry flocks and wild birds, thereby enabling strategic allocation of limited resources for spatial targeting surveillance for AIV in wild birds and poultry.

Materials and Methods

Datasets and Software

We obtained bird-sighting records from the eBird Citizen Science database, the world's largest citizen science program, providing fine-scale occurrence data of bird species (23). The reporting system is based on checklists (22), whereby the observer provides a list of birds detected, GPS location, sampling effort (whether all detected species are reported), sampling duration, sampling protocol (e.g., stationary point, travel, and banding and distance traveled in the case of traveling protocol), starting time of the sampling event, and number of observers. We used the eBird Taiwan dataset focusing on the records from January 2015 through June 2020. The Taiwan Endemic Species Research Institute, Council of Agriculture, Taiwan, established an open terrestrial environmental dataset with 1-km high resolution spanning 5-decade periods during 1970–2020 and used it to predict occupancy probability of the selected wild bird species (24). This dataset contains 100 variables, including 9 land-cover types (e.g., farmland, forest, or wetland), 8 topographies (e.g., latitude or slope), 79 climates (e.g., monthly average temperature or rainfall), and 4 other variables (e.g., traffic or length of roads). From the Council of Agriculture, Taiwan, we obtained the

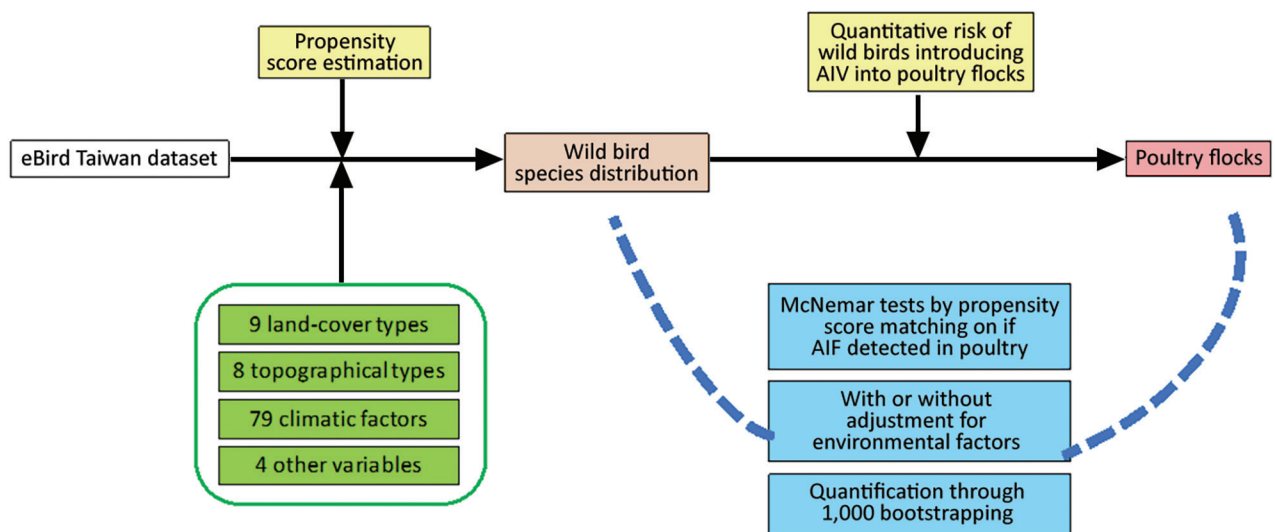


Figure 1. Framework of the analyses performed to map the risk of wild birds introducing avian influenza virus (AIV) into poultry farms for study of integrating citizen scientist data into the surveillance system for avian influenza virus, Taiwan.

complete poultry farm census dataset, established in 2017 and based on an islandwide survey that used remote satellite imaging technology conducted by the Taiwan Agriculture Research Institute. The poultry farm outbreaks dataset was obtained from the surveillance system established by the Bureau of Animal and Plant Health Inspection and Quarantine, Taiwan, as described previously (20,25). During 2015–2017, a total of 1,223 poultry farm outbreaks were reported and laboratory confirmed in Taiwan (1,003 outbreak poultry farms in 2015, 38 in 2016, and 182 in 2017).

We partitioned Taiwan into 4,762 squares, each 3×3 km, consisting of 306 grids, covering the coastline for follow-up spatial modeling. We performed all graphs and statistics in R software (The R Foundation for Statistical Computing, <https://www.R-project.org>) and produced maps by using QGIS (<https://www.qgis.org>). The packages used in R can be found from coding sources provided at http://aiv.nchu.edu.tw/Open_data.html.

Spatial Exploration

To explore the spatial relationship of land-cover types or wild bird distribution, we subjected the area of each land-cover type or propensity score from each grid estimated for individual wild bird species from the wild bird species distribution map to principal component analysis and t-distributed stochastic neighbor embedding (tSNE) analysis. The tSNE analysis is a modern dimension reduction method that uses an iterative algorithm to visualize the high-dimensional data in 2 dimensions while also revealing some global structures (i.e., clusters) (26).

Wild Bird Species Distribution Map

To investigate the risk for AIV exchange at the interface between poultry flocks and wild birds, we first mapped the potential distribution of the wild bird species (Figure 1). All spatial models are based on partitions, which generated 4,762 grids, 3×3 km each. To eliminate spatial counting bias in eBird data, we applied a set of autoregressive logistic models to the eBird Taiwan dataset to estimate the occupancy probability of the distribution of each species of wild bird in each spatial grid (27) (Appendix 1, <https://wwwnc.cdc.gov/EID/article/29/1/22-0659-App1.pdf>). Because multicollinearity might be present, to improve the stability of regression estimation, we used the elastic net method for variable selection. If the zero-inflated Poisson model did not fit the data well, we used the zero-inflated negative binomial regression model instead (28,29). Last, we used the occupancy probability of each bird species

for individual grids to generate the distribution map for individual bird species. The estimated probability of occupancy is the propensity score, which we used for the matched-pair design (30).

Risk Mapping at the Interface of Wild Birds and Poultry

A fundamental problem with mapping the risk for AIV transmission at the interface between wild birds and poultry is the difficulty of quantifying the amount of contact between them. Hence, we measured relative spatial risk on a $3\text{-km} \times 3\text{-km}$ grid by matching on the propensity score the occupancy probability (P_m) of each bird species. The tolerance of matching criterion is $P_m \times 10\%$, which means if the case grid has its estimated score, the matched control should have a score lying within the tolerance interval ($P_{m,l}, P_{m,u}$), in which $P_{m,l} = 0.90$ and $P_{m,u} = \min(1.10, 1)$. We considered the approach of matched-pair design, in which the case grid contains ≥ 1 poultry farm outbreak and the control grid contains poultry farms with no outbreaks during 2015–2017. Because the species of wild bird is both itself a risk factor as well as a confounder, propensity scores for each species with respect to all other species are matched out. By this manner, we estimated the partial effect of that particular species, possibly with adjustment for environmental and terrestrial factors. The association was measured by the McNemar χ^2 statistic on 1 degree of freedom. Because there could be many candidate controls for each case grid, we performed 1,000 bootstrapped resamplings to produce 1,000 -realizations under the null hypothesis that the specific species of bird has no association with the outbreaks. We report the bootstrap results using the notations N_{pa} = number of positive associations in 1,000 replicates and N_{sp} = number of significant positive associations in those N_{pa} experiments (Table). The proportion of N_{sp} can be interpreted as parallel to the concept of p value, if the complement of $(1 - N_{sp}/1,000)$ is taken. The proportion of $N_{sp}/1,000$ reflects the strength against the null hypothesis; higher values imply stronger evidence. However, we did not adopt a strict criterion for statistical significance; that is, we did not require p to be < 0.05 (Appendix 1). We used the proportion of N_{sp} as the probability of AIV being introduced by the wild birds into poultry farms or vice versa.

After matched-pair McNemar analysis, we used only the bird species with positive association to depict a risk map of AIV exchange at the interface between poultry flocks and wild birds. The risk, defined as an infection probability (R_j) of grid j , can be estimated by an additive-multiplicative risk model (Appendix 1).

Table. Risk for avian influenza virus transmission from wild birds to poultry, with and without adjustments for environmental and terrestrial factors*

Wild bird species	Common name	Without adjustment		With adjustment	
		N _{pa}	N _{sp} (in N _{pa})	N _{pa}	N _{sp}
<i>Calidris subminuta</i>	Long-toed stint	998	544	1,000	784(A)
<i>Chroicocephalus ridibundus</i>	Black-headed gull	1,000	896	1,000	482
<i>Tachybaptus ruficollis</i>	Little grebe	976	116	998	402
<i>Gallinago gallinago</i>	Common snipe	944	87	991	191
<i>Anas acuta</i>	Pintail duck	916	18	980	174
<i>Pluvialis fulva</i>	Pacific golden plover	987	171	993	157
<i>Himantopus himantopus</i>	Black-winged stilt	968	138	816	27
<i>Sternula albifrons</i>	Little tern	999	416	964	9
<i>Hirundo rustica</i>	House swallow	956	119	X	X
<i>Bubulcus ibis</i>	Cattle egret	972	188	X	X

*N_{pa}, no. positive associations in 1,000 replicates; N_{sp}, no. significant positive associations in the N_{pa} experiments.

Results

We report all grids with bird-sighting records for 2015–2020 (Figure 2, panel A). There are no records for central grids of Taiwan because they are high-mountain areas and are not easily accessible by bird sighters. Because poultry farms are not distributed in the high-mountain areas (Figure 2, panels B, C), such sparse data did not affect our follow-up analysis.

Occupancy probability was estimated by zero-inflated Poisson model (Figure 3, panel B). The distribution of the predicted occupancy probability is consistent with the bird-sighting distribution from the observer records (Figure 3, panel A) and highly overlaps with the wetland land-cover type (Figure 3, panel C). Distribution maps for all 68 species of wild bird are shown at http://aiv.nchu.edu.tw/migrating_species.html. Among the 68 species, 66 selected for this study can be well modeled for their

occupancy probabilities by using a zero-inflated Poisson model.

The major land-cover type in Taiwan is forest, which comprises 55.8% of the total area of Taiwan's main island, and <0.1% of the area is poultry farms (Figure 4, panel A). On the contrary, <2.5% of main island area is covered by bush, wetland, and bare land, which are the main land-cover types for poultry farming. Water bodies cover only 1.19% of the island but also contain 3.27% of the area for poultry farming, mainly Anseriformes, such as ducks and geese. Because the estimated occupancy probability of wild bird species is based on 4,762 grids, 3-km × 3-km, generated for the whole island, many grids are made of mixed land-cover types (Figure 4, panel B). To explore the relationship of wild bird distribution with land-cover type, the estimated occupancy probabilities, also referred to as propensity scores, of 68 different species of

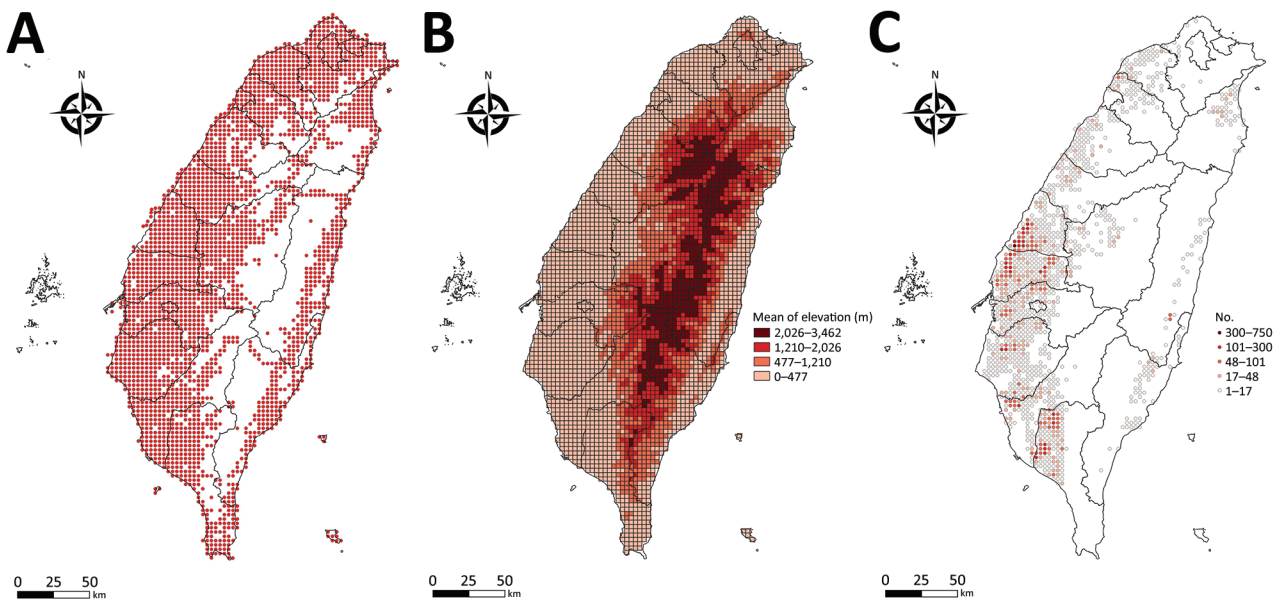


Figure 2. Distribution maps for study of integrating citizen scientist data into the surveillance system for avian influenza virus, Taiwan. A) The 3-km × 3-km grid with bird-sighting records based on Taiwan eBird dataset during 2015–2020; B) average altitude based on Taiwan open terrestrial environmental dataset; C) poultry farm census data for Taiwan.

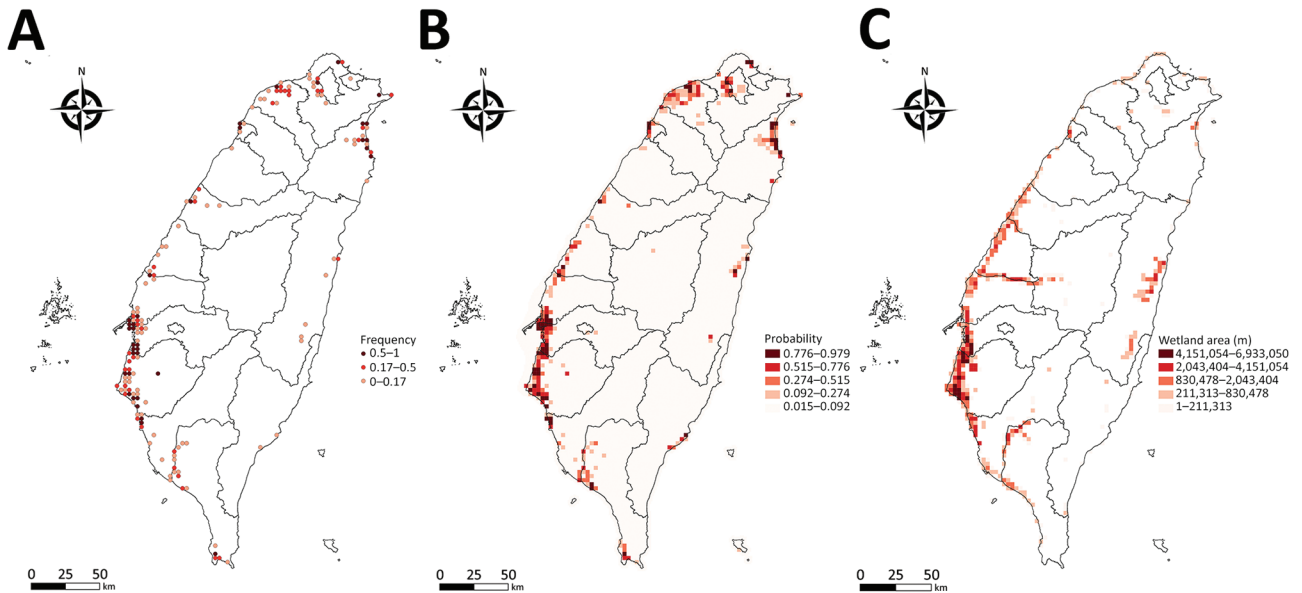


Figure 3. Distribution maps of pintail duck (*Anas acuta*) for study of integrating citizen scientist data into the surveillance system for avian influenza virus, Taiwan. A) True observation frequency from Taiwan eBird dataset; B) occupancy probability estimated by zero-inflated Poisson model; C) distribution map of wetland, based on the land-cover type from the Taiwan open terrestrial environmental dataset.

wild bird were also subjected to principal component analysis and tSNE. The results showed that various wild birds were distributed in different ecologic environments, including forest and bodies of water, for which probabilities for AIV exchange between poultry farms and wild birds might differ (Figure 4, panel C).

In the second stage of our analysis, we performed propensity score matching with bootstrapping to precisely map the probability of AIV exchange between poultry flocks and wild birds. By doing so, we treated environmental factors as confounders and included them for the purpose of multivariate adjustment. Through propensity score matching with the probability of wild bird appearance, the significance of poultry farm outbreaks caused by HPAIV could be examined by bootstrapped resampling scheme based on randomness in selecting case-control matched pairs. There were nonignorable species with ≥ 100 significant results among the 1,000 bootstrapped realizations of the McNemar statistic (Table 1). Four species of wild bird, including the long-toed stint, black-headed gull, little grebe, and pacific golden plover, were highly correlated with the HPAIV outbreaks on poultry farms, with or without adjustment. The wild bird species that can be viewed as being significant when environmental factors were considered, is the long-toed stint, with a p value of 0.216 (1 - 0.784) (Table 1). On the other hand, if environmental factors were not considered, the black-headed gull shows a highly significant association ($p = 1 - 0.896 = 0.104$).

Discussion

The continuing circulation and reassortment of Gs/Gd-like HPAIV with LPAIV has caused huge economic losses and raised public health concerns because of its zoonotic potential (31). Virologic surveillance of wild birds has been suggested as part of a global AIV surveillance system (32,33) and could directly benefit human and animal health through knowledge of how avian influenza virus genes flow among different hosts and how factors that drive AIV prevalence in wild birds enable virus spillover, emergence, and maintenance. However, problems with understanding the transmission and evolution of HPAIV include underreporting, biased selection of sampling sites, and limiting AIV surveillance to wild bird carcasses (34). The risk map generated in this study (Figure 5) can be used for, but is not limited to, educational purposes of the government to communicate with stakeholders to increase their biosecurity of poultry farms; a sustained cost-effective AIV surveillance program that promotes sampling site selections, thereby enabling limited resources to be strategically allocated for early detection of changing AIV dynamics in reservoir populations to support public health and pandemic preparedness (35); and a quantitative assessment of the risk of introducing AIV from wild birds into poultry flocks as well as the possible transmission of AIVs between wild bird populations affected by bird behavior, age structures of populations, and detailed migration routes.

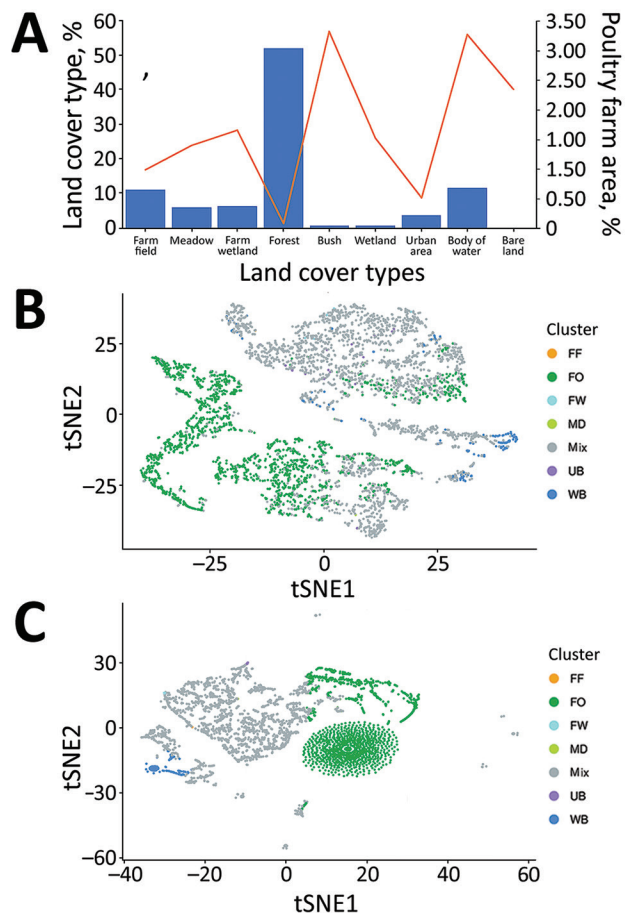


Figure 4. Land cover and bird distribution data for study of integrating citizen scientist data into the surveillance system for avian influenza virus, Taiwan. A) Percentages of 9 land-cover types in the total area of Taiwan main island (bars), area of poultry farms in the total area of indicated land-cover types (line). B, C) The clustering pattern of the area of each land-cover type (B) and the propensity score for each bird species from 3,764 grids partitioned by 3-km \times 3-km squares of the main island of Taiwan (C), are based on principal component analysis and tSNE dimension reduction. Clusters are colored by the land-cover type as shown in panel A. For 4,762 grids, if 1 specific land-cover type is composed of >90% in the grid, such grid will be regarded as such specific land-cover type. Otherwise, it will be labeled as the mixed land-cover type. The labels of clusters in panels B and C are consistent with those in panel A. FF, farm field; FO, forest; FW, farm wetland; MD, meadow; mix, mixed land-cover types; tSNE, t-distributed stochastic neighbor embedding; UB, urban; WB, water body.

Pathogens that cross the interface between diverse populations, such as wildlife and livestock or animals and humans, pose particular challenges to developing effective and efficient surveillance and control measures. AIVs can spread globally among wild birds, poultry, and humans, with potentially devastating effects. The Citizen Science project eBird, which collects large volumes of data across broad spatial and temporal dimensions, provides a great

opportunity for investigating how wild birds contribute to this spread. However, citizen science data often suffer from bias arising from bird sighters' viewing preferences, convenience (for bird sighting and travel planning), incentives (if any), and others. It may even come from the process of data recording and reporting. Although different analytical approaches for minimizing the bias have been published (36–38), our study used a high-quality inventory filtering procedure by constraining aspects of the observation process (e.g., the duration of observation and records of bird species sighting by ignoring the counts of birds on the checklists to remove potential sources of variation and facilitate subsequent analysis). Furthermore, birds are observed mostly during the day, and wild birds may forage near waterfowl poultry farms during the night (39). Such foraging flight distance is relatively short (e.g., the median for pintail ducks marked with satellite transmitters is within 3 km) and is covered by the size of the grids here (C.-C. Chen, National Pingtung University of Science and Technology, pers. comm., 2022 Jul 1).

Another layer of bias in using the eBird dataset comes from the accessibility of bird sighting by the observers. Because the locations for bird sighting are highly influenced by the proximity to the road accessible by the observers, the distribution of bird-sighting records cannot fully reflect the ecologic distribution of the wild birds. However, the main difficulty with building a unified regression model to map the ecologic distribution of wild birds and using the eBird dataset is the number of variables from the open terrestrial environmental dataset. In our study, the numbers of bird species and environmental variables both exceed 100. Therefore, we focused on 1 species at a time but kept all other variables as confounders. The elastic net regularization method was first used as a unified machine learning algorithm to generate parsimonious models for estimating potential risk maps (40). The elastic net regularization method is a compromise between ridge regression and lasso regression. To avoid complexity, we modeled only the presence or absence of individual bird species in each grid by using a conditional autoregressive logistic model, taking spatial autocorrelations into account.

Wild waterfowl are known reservoirs for LPAIV and potentially HPAIV because of the global evolution and circulation of Gs/GD-derived clade 2.3.4.4 (41), which resulted in a new era of AIV surveillance requiring identification of critical interfaces between wild birds and poultry on the landscape for potential interspecies transmission and virus evolution. Although such estimates can be extrapolated from

active poultry surveillance, as suggested by previous studies (42–44), accurately determining the likelihood (or potency) of the exchange of AIV at the interface between poultry flocks and wild birds is difficult because of incomplete active surveillance and a lack of biosecurity information for individual farms. In this study, we performed propensity score matching with bootstrapping by ensuring the randomness of case-control pair selections for estimating probability (45). By doing so, environmental factors were seen as confounders for which further adjustment can be made. We identified 10 nonignorable species of wild bird with ≥ 100 significant results among the 1,000 bootstrapped realizations of the McNemar statistic (Table 1). Among them, 4 wild bird species, including the long-toed stint, black-headed gull, little grebe, and pacific golden plover, were highly correlated with the introduction of HPAIV into poultry farms, with or without adjustment (Table 1). Those 4 species are mainly wintering birds; their preferred habitats are wetland or farmland. In particular, based on GISAID (<https://www.gisaid.org>), there are extensive records of LPAI in black-headed gull, little grebe, and pacific golden plover, which increases their chances of transmitting AIV into poultry farms as shown for the bootstrapping results (Table 1). Although the p values are not high, note that the term “p value” used here represents a concept of significance level based on bootstrapped samples, rather than the 0.05 level of significance criterion traditionally pursued in statistics.

The key limitation of our study is the lack of detailed information contributing to between-farm AIV transmission. Such information includes bridge bird species on or near poultry farms, transportation vehicles, or other farm animals (e.g., rats feeding on bird carcasses). It is also evident that different AIV subtypes and pathotypes can vary according to the epidemiology and prevalence of wild birds (46). For example, the following can interfere with significance results in McNemar tests: spatiotemporal variation in between-farm transmission by wild birds, species age structure, behaviors including roosting/breeding sites, AIV susceptibility, and AIV pathology. Although phylogenetic analysis of HPAIV from individual outbreak poultry farms could reveal between-farm transmission events, we, unfortunately, had no access to sequence data of outbreak viruses. We also selected 36 different nonmigratory wild birds and followed the same analytical frameworks as those for migratory birds. The results suggested that 4 nonmigratory wild bird species, including the black bulbul, black-headed munia, red collared

dove, and common moorhen, could potentially serve as bridging species for introducing AIV into poultry farms (Appendix 2 Table 2, <https://wwwnc.cdc.gov/EID/article/29/1/22-0659-App2.pdf>), although other bridging species could also play major roles. Furthermore, increased occurrence of HPAI in wild birds resulted in disease and death of fairly large numbers of birds ($>10,000$ individuals) and affected diverse species (47). Mortality data for birds, especially nonmigratory species, could be indicators for

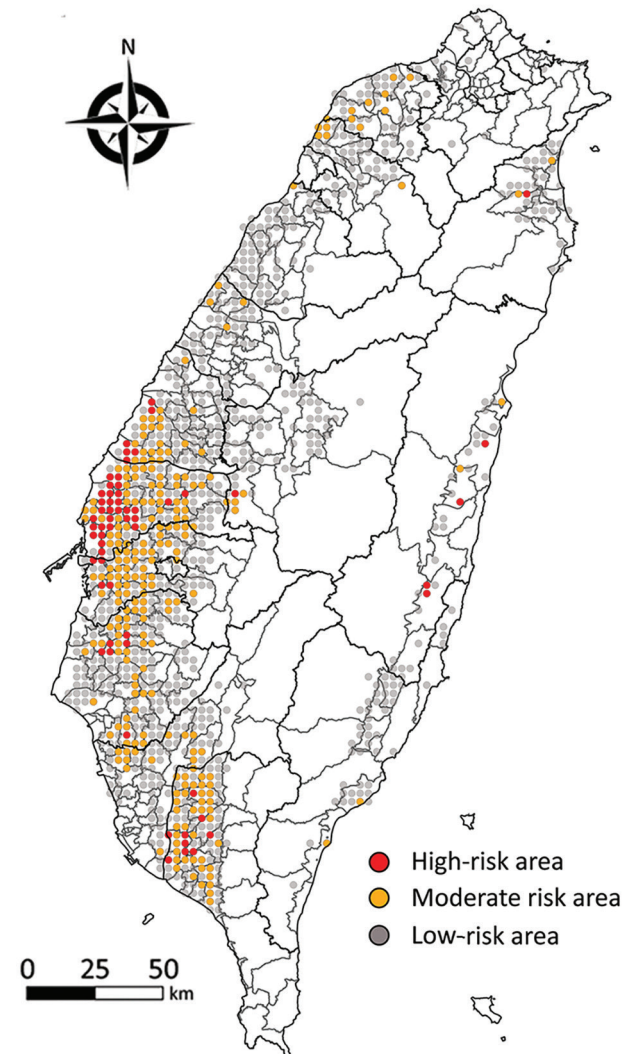


Figure 5. Risk maps showing risk of poultry farm acquiring avian influenza virus infection from migratory wild birds, from study of integrating citizen scientist data into the surveillance system for avian influenza virus, Taiwan. Each dot represents each 3-km \times 3-km grid. Red dots represent the high-risk area with probability calculated based on 10 bird species with high risk of transmitting avian influenza virus into poultry farms (Table). Orange dots represent the middle-risk area, with bird species with ≥ 1 positive McNemar test result. Gray dots represent the low-risk area with bird species having no positive or negative McNemar test results.

HPAIV transmission and could be incorporated into spatiotemporal data analysis together with other genetic or bird behavior data in the future (25).

In summary, information about the spatial distribution of wild birds and how they exchange AIV with poultry, as well as the related risks, has the potential to benefit surveillance, pandemic preparedness, and prevention plans. However, poor availability of data presents challenges. The integration of citizen science data, such as eBird, into the surveillance system is underappreciated, and the workflow developed in our study can be applied in other countries for AIV surveillance in wild bird site selections to increase the breadth of virus strain coverage and knowledge of gene flow of AIV among wild birds.

Acknowledgment

We express our deepest appreciation to A.Y. Chang and W.J. Chen for advice with regard to the eBird dataset. We thank Lydia Wang for English editing of the manuscript and Zheng-Fu Liu and Yong-Sheng Zhuang for their help with statistical computation.

Mountain Jade Scholar Charles W. Tu for provided funding from the ENABLE center of National Chung-Hsing University. The work is also funded by the Bureau of Animal and Plant Health Inspection and Quarantine (110AS-5.5.3-BQ-B1(2)). The funding source of this study had no role in the study design, data collection, data analysis, data interpretation, or writing of the report. The corresponding author had full access to all data in the study and final responsibility for the decision to submit for publication.

The authors declare no conflict of interest of any form that might be perceived to influence the results or discussion reported in this paper.

About the Author

Dr. Wu is an associate professor of statistics in the Department of Applied Mathematics and Institute of Statistics, National Chung Hsing University, Taichung, Taiwan. His research interests include spatial statistics and modeling, epidemiologic study design, and big data analytics.

References

1. Yoon SW, Webby RJ, Webster RG. Evolution and ecology of influenza A viruses. *Curr Top Microbiol Immunol*. 2014;385:359–75. https://doi.org/10.1007/82_2014_396
2. Lee DH, Criado MF, Swayne DE. Pathobiological origins and evolutionary history of highly pathogenic avian influenza viruses. *Cold Spring Harb Perspect Med*. 2021;11:a038679. <https://doi.org/10.1101/cshperspect.a038679>
3. Briand F-X, Niqueux E, Schmitz A, Martenot C, Cherbonnel M, Massin P, et al. Highly pathogenic avian influenza A(H5N8) virus spread by short- and long-range transmission, France, 2016–17. *Emerg Infect Dis*. 2021;27:508–16. <https://doi.org/10.3201/eid2702.202920>
4. Li YT, Linster M, Mendenhall IH, Su YCF, Smith GJD. Avian influenza viruses in humans: lessons from past outbreaks. *Br Med Bull*. 2019;132:81–95. <https://doi.org/10.1093/bmb/ldz036>
5. Smith GJ, Donis RO; World Health Organization/World Organisation for Animal Health/Food and Agriculture Organization (WHO/OIE/FAO) H5 Evolution Working Group. Nomenclature updates resulting from the evolution of avian influenza A(H5) virus clades 2.1.3.2a, 2.2.1, and 2.3.4 during 2013–2014. *Influenza Other Respir Viruses*. 2015;9:271–6. <https://doi.org/10.1111/irv.12324>
6. Lee DH, Bertran K, Kwon JH, Swayne DE. Evolution, global spread, and pathogenicity of highly pathogenic avian influenza H5Nx clade 2.3.4.4. *J Vet Sci*. 2017;18(S1):269–80. <https://doi.org/10.4142/jvs.2017.18.S1.269>
7. Lycett SJ, Pohlmann A, Staubach C, Caliendo V, Woolhouse M, Beer M, et al.; Global Consortium for H5N8 and Related Influenza Viruses. Genesis and spread of multiple reassortants during the 2016/2017 H5 avian influenza epidemic in Eurasia. *Proc Natl Acad Sci U S A*. 2020;117:20814–25. <https://doi.org/10.1073/pnas.2001813117>
8. Global Consortium for H5N8 and Related Influenza Viruses. Role for migratory wild birds in the global spread of avian influenza H5N8. *Science*. 2016;354:213–7. <https://doi.org/10.1126/science.aaf8852>
9. Poulson RL, Brown JD. Wild bird surveillance for avian influenza virus. *Methods Mol Biol*. 2020;2123:93–112. https://doi.org/10.1007/978-1-0716-0346-8_8
10. Prosser DJ, Hungerford LL, Erwin RM, Ottinger MA, Takekawa JY, Newman SH, et al. Spatial modeling of wild bird risk factors for highly pathogenic A(H5N1) avian influenza virus transmission. *Avian Dis*. 2016;60 (Suppl):329–36. <https://doi.org/10.1637/11125-050615-Reg>
11. Hill A, Gillings S, Berriman A, Brouwer A, Breed AC, Snow L, et al. Quantifying the spatial risk of avian influenza introduction into British poultry by wild birds. *Sci Rep*. 2019;9:19973. <https://doi.org/10.1038/s41598-019-56165-9>
12. Prosser DJ, Hungerford LL, Erwin RM, Ottinger MA, Takekawa JY, Ellis EC. Mapping avian influenza transmission risk at the interface of domestic poultry and wild birds. *Front Public Health*. 2013;1:28. <https://doi.org/10.3389/fpubh.2013.00028>
13. La Sala LF, Burgos JM, Blanco DE, Stevens KB, Fernández AR, Capobianco G, et al. Spatial modelling for low pathogenicity avian influenza virus at the interface of wild birds and backyard poultry. *Transbound Emerg Dis*. 2019;66:1493–505. <https://doi.org/10.1111/tbed.13136>
14. Franklin AB, Bevins SN, Ellis JW, Miller RS, Shriner SA, Root JJ, et al. Predicting the initial spread of novel Asian origin influenza A viruses in the continental USA by wild waterfowl. *Transbound Emerg Dis*. 2019;66:705–14. <https://doi.org/10.1111/tbed.13070>
15. Tian H, Zhou S, Dong L, Van Boeckel TP, Cui Y, Newman SH, et al. Avian influenza H5N1 viral and bird migration networks in Asia. *Proc Natl Acad Sci U S A*. 2015;112:172–7. <https://doi.org/10.1073/pnas.1405216112>
16. Wood C, Sullivan B, Iliff M, Fink D, Kelling S. eBird: engaging birders in science and conservation. *PLoS Biol*. 2011;9:e1001220. <https://doi.org/10.1371/journal.pbio.1001220>
17. Callaghan CT, Nakagawa S, Cornwell WK. Global abundance estimates for 9,700 bird species. *Proc Natl Acad*

- Sci U S A. 2021;118:e2023170118. <https://doi.org/10.1073/pnas.2023170118>
18. Kelling S, Johnston A, Hochachka WM, Iliff M, Fink D, Gerbracht J, et al. Can observation skills of citizen scientists be estimated using species accumulation curves? *PLoS One*. 2015;10:e0139600. <https://doi.org/10.1371/journal.pone.0139600>
 19. Boakes EH, Gliozzo G, Seymour V, Harvey M, Smith C, Roy DB, et al. Patterns of contribution to citizen science biodiversity projects increase understanding of volunteers' recording behaviour. *Sci Rep*. 2016;6:33051. <https://doi.org/10.1038/srep33051>
 20. Liang W-S, He Y-C, Wu H-D, Li Y-T, Shih T-H, Kao G-S, et al. Ecological factors associated with persistent circulation of multiple highly pathogenic avian influenza viruses among poultry farms in Taiwan during 2015-17. *PLoS One*. 2020;15:e0236581. <https://doi.org/10.1371/journal.pone.0236581>
 21. Lee MS, Chen LH, Chen YP, Liu YP, Li WC, Lin YL, et al. Highly pathogenic avian influenza viruses H5N2, H5N3, and H5N8 in Taiwan in 2015. *Vet Microbiol*. 2016;187:50-7. <https://doi.org/10.1016/j.vetmic.2016.03.012>
 22. Sullivan BL, Aycrigg JL, Barry JH, Bonney RE, Bruns N, Cooper CB, et al. The eBird enterprise: an integrated approach to development and application of citizen science. *Biol Conserv*. 2014;169:31-40. <https://doi.org/10.1016/j.biocon.2013.11.003>
 23. Sullivan BL, Wood CL, Iliff MJ, Bonney RE, Fink D, Kelling S. eBird: a citizen-based bird observation network in the biological sciences. *Biol Conserv*. 2009;142:2282-92. <https://doi.org/10.1016/j.biocon.2009.05.006>
 24. Chen WJ, Lo CC, Tsai FA, Chang AY. Using open data to establish a multi-temporal and terrestrial environmental dataset of Taiwan [in Chinese]. *Taiwan Journal of Biodiversity*. 2020;22:13-44.
 25. Wu H-D I, Chao D-Y. Two-stage algorithms for visually exploring spatio-temporal clustering of avian influenza virus outbreaks in poultry farms. *Sci Rep*. 2021;11:22553. <https://doi.org/10.1038/s41598-021-01207-4>
 26. Van der Maaten L, Hinton G. Visualizing data using t-SNE. *Journal of Machine Learning Research*. 2008;9:2579-605.
 27. Anselin L. *Spatial econometrics: methods and models*. Dordrecht: Kluwer Academic Publishers. 1988.
 28. Lord D, Washington SP, Ivan JN. Poisson, Poisson-gamma and zero-inflated regression models of motor vehicle crashes: balancing statistical fit and theory. *Accid Anal Prev*. 2005;37:35-46. <https://doi.org/10.1016/j.aap.2004.02.004>
 29. Lambert D. Zero-inflated Poisson regression, with an application to defects in manufacturing. *Technometrics*. 1992;34:1-14. <https://doi.org/10.2307/1269547>
 30. Rosenbaum PR, Rubin DB. The central role of the propensity score in observational studies for causal effects. *Biometrika*. 1983;70:41-55. <https://doi.org/10.1093/biomet/70.1.41>
 31. Yamaji R, Saad MD, Davis CT, Swayne DE, Wang D, Wong FYK, et al. Pandemic potential of highly pathogenic avian influenza clade 2.3.4.4 A(H5) viruses. *Rev Med Virol*. 2020;30:e2099. <https://doi.org/10.1002/rmv.2099>
 32. Machalaba CC, Elwood SE, Forcella S, Smith KM, Hamilton K, Jebara KB, et al. Global avian influenza surveillance in wild birds: a strategy to capture viral diversity. *Emerg Infect Dis*. 2015;21:e1-7. <https://doi.org/10.3201/eid2104.141415>
 33. Verhagen JH, Fouchier RAM, Lewis N. Highly pathogenic avian influenza viruses at the wild-domestic bird interface in Europe: future directions for research and surveillance. *Viruses*. 2021;13:212. <https://doi.org/10.3390/v13020212>
 34. Olsen B, Munster VJ, Wallensten A, Waldenström J, Osterhaus AD, Fouchier RAM. Global patterns of influenza A virus in wild birds. *Science*. 2006;312:384-8. <https://doi.org/10.1126/science.1122438>
 35. Cheng MC, Lee MS, Ho YH, Chyi WL, Wang CH. Avian influenza monitoring in migrating birds in Taiwan during 1998-2007. *Avian Dis*. 2010;54:109-14. <https://doi.org/10.1637/8960-061709-Reg.1>
 36. Xue Y, Davies I, Fink D, Wood C, Gomes CP. Avicaching: a two-stage game for bias reduction in citizen science. In: *Proceedings of the 15th International Conference on Autonomous Agents and Multiagent Systems*; 2016 May 9-13; Singapore. p. 776-85.
 37. Chen D, Gomes CP. Bias reduction via end-to-end shift learning: application to citizen science. *Proc Conf AAAI Artif Intell*. 2019;33:493-500. <https://doi.org/10.1609/aaai.v33i01.3301493>
 38. Troudet J, Grandcolas P, Blin A, Vignes-Lebbe R, Legendre F. Taxonomic bias in biodiversity data and societal preferences. *Sci Rep*. 2017;7:9132. <https://doi.org/10.1038/s41598-017-09084-6>
 39. Elbers ARW, Gonzales JL. Quantification of visits of wild fauna to a commercial free-range layer farm in the Netherlands located in an avian influenza hot-spot area assessed by video-camera monitoring. *Transbound Emerg Dis*. 2020;67:661-77. <https://doi.org/10.1111/tbed.13382>
 40. Zou H, Hastie T. Regularization and variable selection via the elastic net. *J R Stat Soc B*. 2005;67:301-20. <https://doi.org/10.1111/j.1467-9868.2005.00503.x>
 41. He G, Ming L, Li X, Song Y, Tang L, Ma M, et al. Genetically divergent highly pathogenic avian influenza A(H5N8) viruses in wild birds, eastern China. *Emerg Infect Dis*. 2021;27:2940-3. <https://doi.org/10.3201/eid2711.204893>
 42. Gonzales JL, Stegeman JA, Koch G, de Wit SJ, Elbers ARW. Rate of introduction of a low pathogenic avian influenza virus infection in different poultry production sectors in the Netherlands. *Influenza Other Respir Viruses*. 2013;7:6-10. <https://doi.org/10.1111/j.1750-2659.2012.00348.x>
 43. Bouwstra R, Gonzales JL, de Wit S, Stahl J, Fouchier RAM, Elbers ARW. Risk for low pathogenicity avian influenza virus on poultry farms, the Netherlands, 2007-2013. *Emerg Infect Dis*. 2017;23:1510-6. <https://doi.org/10.3201/eid2309.170276>
 44. Gonzales JL, Pritz-Verschuren S, Bouwstra R, Wiegel J, Elbers ARW, Beerens N. Seasonal risk of low pathogenic avian influenza virus introductions into free-range layer farms in the Netherlands. *Transbound Emerg Dis*. 2021;68:127-36. <https://doi.org/10.1111/tbed.13649>
 45. Efron B. Bootstrap methods: another look at the jackknife. *Ann Stat*. 1979;7:1-26. <https://doi.org/10.1214/aos/1176344552>
 46. Li Y-T, Chen C-C, Chang A-M, Chao D-Y, Smith GJ. Co-circulation of both low and highly pathogenic avian influenza H5 viruses in current poultry epidemics in Taiwan. *Virus Evolution*. 2020;6:veaa037.
 47. Ramey AM, Hill NJ, DeLiberto TJ, Gibbs SEJ, Hopkins MC, Lang AS, et al. Highly pathogenic avian influenza is an emerging disease threat to wild birds in North America. *J Wildl Manage*. 2022;86:e22171. <https://doi.org/10.1002/jwmg.22171>

Address for correspondence: Day-Yu Chao, Graduate Institute of Microbiology and Public Health, College of Veterinary Medicine, National Chung-Hsing University, Taichung 402, Taiwan; email: dychao@nchu.edu.tw

Integration of Citizen Scientist Data into the Surveillance System for Avian Influenza Virus, Taiwan

Appendix

Part I: eBird dataset and wildbird species selection

Taiwan, on the East Asian route of bird migration, launched the eBird Taiwan program in 2015 and has since accumulated over 4,800 users by February 2022, who have contributed stable bird sighting checklists since 2015. After removing repeated checklists, a total of 336,154 checklists with 3,778,382 numbers of wild bird species recorded from each checklist were found in Taiwan the ebird dataset between January 2015 and June 2020, Multiple observations of the same birds can happen either because several observers travelled together or because they came independently to the same site on the same day, both situations creating pseudo-replication. Therefore, we only consider the presence or absence of wild bird species observed here.

To avoid reporting bias commonly found from citizen science dataset, we filtered the dataset with the three different criteria to obtain high-quality checklists comparable in amounts of efforts. The criteria include: (i) the traveling distance was less than 2 kilometers, otherwise they may not represent the local bird composition around the reported GPS location (*l*), (ii) the observation area was less than 100 hectares to ensure the identified bird species fell into 3km×3km grids, and (iii) the duration of continuous observation was limited to ≤ 240 minutes

since the duration exceed this criterion tends to correlate with particular bird sighting activity, such as Taiwan New Year bird count event (2). We didn't restrict the checklists based on the sampling protocol of the observers used since we are trying to capture all bird sighting activities regardless of whether the observers would record all species or target only specific bird species. After data filtering, we obtained the final dataset used for the analysis, which consisted of 2,366,327 records of total numbers of species, covering 735 species, from 3080 observers.

Wildbird species selection

Before constructing the wild bird distribution map, the initial step is the selection of wild bird species relevant for the introduction of either HPAI or LPAI into the poultry farm. The bird species which show passage or regularly occurring breeding and wintering with preference to areas in Taiwan, and passing once or twice a year, may potentially act as a reservoir for LPAI, and will thus be considered for selection. The final inclusion criteria of bird species was based on either the top 20% abundancy by ranking the counts from the checklists of the observers (3) or the influenza virus isolation records from 3 databases: Influenza Virus Database-NCBI (<https://www.ncbi.nlm.nih.gov/genomes/FLU/Database/nph-select.cgi>), EMPRES-I (<https://empres-i.apps.fao.org/>) and Influenza Research Database (IRD) (<https://www.fludb.org/brc/home.spg?decorator=influenza>) before the date of 12/03/2020. In total, 68 species of wild birds were included in this study, including 22 species selected which are ranked on the top 20% observations with a minimum of >100,000 being defined as “substantially” abundant. Appendix 2 Table 1 (<https://wwwnc.cdc.gov/EID/article/29/1/22-0659-App2.pdf>) summarizes the complete list of bird species with their scientific name and common names under international taxonomy based on the second edition of the Avifauna of Taiwan or Avibase (<https://avibase.bsc-eoc.org/avibase.jsp>).

Part II: Estimating the occupancy risk map

Variable selection

The main difficulty in building a universally valid regression is that the presence (or absence) of bird species involves many variables (including land-related factors and environmental variables). It is challenging to obtain a unified explanation about the model structure. To estimate a risk map (occupancy probability), a variable selection procedure, called the *elastic net* method, were used for screening significant variables, including bird species and environmental factors. The elastic net method is a compromise between ridge regression and Lasso (4,5).

Defining the resolution: 3km×3km grids

Let Taiwan be divided into a set of 3km×3 km grids, each with an area equal to 9 km², with four sides parallel to the Earth's longitudes and latitudes. This partition gives 4,762 grids covering the entire map of Taiwan including the coastline. Let the squares be denoted as $A_1^*, A_2^*, \dots, A_{N^*}^*$ ($N^*=4,762$). Because not all $\{A_i^*\}_{i=1}^{N^*}$ (denoted as \mathcal{A}^*) include both bird observations and poultry farms, let $\mathcal{A} = \{A_i\}_{i=1}^N$ denote a subset of $\{A_i^*\}_{i=1}^{N^*}$, where \mathcal{A} includes only those with both farms and birds observation records ($N=1,073$). Hereafter we call \mathcal{A} *the matrix of grids with bird observations*. Note that the grids in $\mathcal{A}^* \setminus \mathcal{A}$ that contain no poultry farms are the ones located at or near elevated mountain areas. Let $y_{i,k}^*$ be the number of birds of species k reported in the i -th grid; $y_{i,k} = \mathbf{1}\{y_{i,k}^* \geq 1\}$ is the indicator of whether there is any observation of k -species in that i -th grid; $k=1, \dots, K$ with K being the total number of species. Further, let $t_{i,k,s}$ be the value of the s -th variable for temporal, terrestrial, and environmental factors.

Modeling the occupancy

For species k , we first estimate the probability of its occurrence based on the presence or absence of other species as explanatory variables. This probability, denoted U and interpreted as a propensity score, is used as the “matching variable” in the following text. To model outbreaks in grids containing a certain number of poultry farms, the presence or absence of species k was used as the primary explanatory variable when the corresponding propensity scores U were matched. Therefore, it is still necessary to estimate the probability of occurrence of each species of bird in each grid based on a logistic autoregressive model to present an overall risk map.

Notations and model description

For grid “ i ” and for bird species “ k ”, $Y_{i,k}$ is the indicator variable of existence of species “ k ”, and $Y_{i,-k}$ is the indicator of all other species than species k . A natural conclusion is: the existence of species k depends on all the other species; and thus $Y_{i,-k}$ is a $(K-1)$ -dimensional vector. Besides, $T_{i,k}$ is the vector-valued variable representing all other variables (including the environmental data) except for bird species. Explicit modeling of spatial correlation between Y and the other T s is implemented through the variable $Y_{-i,k}$, which is also an indicator variable of observing species k in all adjacent grids using Queen’s contiguity-based neighbors (6), that is $Y_{-i,k} = 1$ (I), where A is the event of $\sum_{\{-i\}} Y_{i,k} \geq 1$ when summed around grid “ i ”, denoted by the set $\{-i\}$.

The ZIP model estimates the probability of bird occupancy in a grid that accommodates both structural zeros (species never appear in the grid) and random zeros:

$$\log(\lambda_{i,k}) = \beta_0 + Y_{i,-k}'\beta + T_{i,k}'\gamma + \phi Y_{-i,k}, \quad (A1)$$

$$\log\left(\frac{\alpha_{i,k}}{1-\alpha_{i,k}}\right) = \theta_0 + Y_{i,-k}'v. \quad (A2)$$

Estimating occupancy probabilities using autoregressive logistic model

The principle of incorporating spatial autocorrelation is to consider the correlation with adjacent grids. Let $P(Y_{i,k} = 1|Y_{i,-k}, T_{i,k}, Y_{-i,k})$ be the occupancy probability given the “status” of the adjacent grids and the other land-cover and environmental variables. Explicit modeling of spatial correlation between Y and the other T is implemented through the variable $Y_{-i,k}$ which is an indicator of observing species k in all adjacent grids (using Queen’s contiguity-based neighbors).

$$\log\left(\frac{P(Y_{i,k} = 1|Y_{i,-k}, T_{i,k}, Y_{-i,k})}{1-P(Y_{i,k} = 1|Y_{i,-k}, T_{i,k}, Y_{-i,k})}\right) = \beta_0 + Y_{i,-k}'\beta + T_{i,k}'\gamma + \phi Y_{-i,k} \quad (A3)$$

The occupancy probability is estimated through a ZIP model by summing the probabilities of nonzero terms:

$$P(y_{i,k} = 0) = (1 - \alpha_{i,k}) + \alpha_{i,k}e^{-\lambda_{i,k}} \quad (A4)$$

In (A3), the advantage of using the indicator metric $Y_{i,-k}$ to model occupancy is that it avoids possible biases based on intrinsic properties of the eBird data, which can arise when reporting the number of species observed, but less often happens when only occupancy "status" is adopted. However, reducing bias inevitably leads to a loss of efficiency in statistical estimation. In the event the ZIP model is not suitable for model fitting, the zero-inflated negative binomial (ZINB) model can be used instead (7).

Propensity score and matched-pair design

The propensity score (U) corresponding to an indicator variable Z , which is random but dependent on a set of covariates, is the (estimated) probability of being equal to 1 for Z . To the purpose of adjustment for multiple explanatory variables (denoted by \mathbf{X}) in this study, we consider \mathbf{X} to include the indicators of observing species other than bird species k , as well as

many other variables. After the adjustment (for the propensity score), the risk factors are re-assessed for their association with the outcome variable (Y) by matching on the propensity score (8). The remaining question is: why use propensity score matching? First, the variable number of bird species can be large, making it impractical to report the risk of individual bird species one-by-one. Because of this concern, we consider the approach of matched-pair design so that the propensity scores of each species relative to all other species are matched. In addition, through this setting, the adjustment of environmental factors can also be achieved.

How to construct the case-control set

Among the $N=1,073$ grids where bird observations were reported, there are $D=296$ grids which contains at least 1 outbreak. We call the grid in D a “case”, and for the other $C=N-D=777$ grids where no outbreak was reported, we call them “controls”. In the sequel, we denote S_D as the set of “case” grids, and S_C as the set of “control” grids. Since every case can have multiple matched controls, it is possible to consider a resampling scheme from the matched control set and compute the McNemar statistic for each resampling.

McNemar’s matched-pair association test and Bootstrapping

For a cell in S_D , and according to the *propensity* of each bird species estimated in the aforementioned grid, we use U_d to represent the potential of this grid according to a certain ordering method, $d=1, \dots, D$. We look for matched control for each case grid in the following manner: Let U_c represent the propensity of the bird species calculated by the grid in the control set S_C , then $M_{c(d)} = (P_{m,l}, P_{m,u})$, where $P_{m,l}$ and $P_{m,u}$ are stated in the “Materials and Methods” Section.

In the Appendix Table, let $\vartheta_d^{(k)} = 1$ if there is an observation record of the k -th bird species in at least one grid in S_D ; otherwise $\vartheta_d^{(k)} = 0$. On the other hand, for the control grid

randomly selected out of the corresponding S_C subset $M_{c(d)}$, if this grid has an observation record of the k -th species, then $\vartheta_{c(d)}^{(k)} = 1$; otherwise $\vartheta_{c(d)}^{(k)} = 0$.

Appendix 1 Table. Forming McNemar chi-square tests from a matched-pair 2 by 2 table.

Condition (ii) ↓		Condition (i) →	
		A cell randomly selected from $M_{c(d)}$ has species k ?	
		Yes	No
Cell d in S_D has species k	Yes	$\vartheta_d^{(k)} \times \vartheta_{c(d)}^{(k)}$	$\vartheta_d^{(k)} \times (1 - \vartheta_{c(d)}^{(k)})$
	No	$(1 - \vartheta_d^{(k)}) \times \vartheta_{c(d)}^{(k)}$	$(1 - \vartheta_d^{(k)}) \times (1 - \vartheta_{c(d)}^{(k)})$

In these four yes-no cells, only one of them equals to 1, the other three equal to 0. Here a “one” represents “one matched-pair”. Taking the summation over $d=1, \dots, D$, we obtain the total number of discordant pairs. Further, let $\alpha^{(k)}$ be the number of pairs that the case grid has species- k but the control-grid does not;

$$\alpha^{(k)} = \sum_{d=1}^D \vartheta_d^{(k)} \times (1 - \vartheta_{c(d)}^{(k)}), \quad \beta^{(k)} = \sum_{d=1}^D (1 - \vartheta_d^{(k)}) \times \vartheta_{c(d)}^{(k)}. \quad (A5)$$

Conversely, $\beta^{(k)}$ is the number of pairs that the case-grid has no species- k but the control-grid does have. Because the random sampling is implemented on $M_{c(d)}$, a subset of S_C , the bootstrapping suggests that this random sampling can be repeated B times for a large “ B ” (9). If, temporarily, the number of poultry farm in the cells are not taken into account (but actually the number itself is a risk factor of the outbreak indicator of that cell), denote $\alpha_b^{(k)}$ and $\beta_b^{(k)}$ to be the numbers of discordant pairs with conditions (i) and (ii) stated above for species k , and at the b -th resampling. Let $\chi_b^{(k)}$ be the realization of McNemar statistic calculated at the b -th resampling:

$$\chi_b^{(k)} = \frac{(|\alpha_b^{(k)} - \beta_b^{(k)}| - 1)^2}{\alpha_b^{(k)} + \beta_b^{(k)}}, \quad b=1, 2, \dots, B \quad (A6)$$

The McNemar statistic in (A6) only provides a measure of significance, so we need to further consider the issue of positive or negative association.

Let $\text{sign}(\alpha_b^{(k)} - \beta_b^{(k)})$ denote the indicator of positive or negative association between the k-th species and the outbreak event. Using $1_{\{\alpha_b^{(k)} > \beta_b^{(k)}\}}$ and $1_{\{\alpha_b^{(k)} \leq \beta_b^{(k)}\}}$ to represent the indicator of positive or negative association, respectively, in the b-th replication of the bootstrapping procedure, we have (for b=1 to B):

$$p^{(k)} = \frac{1}{B} \sum_{b=1}^B 1_{\{\alpha_b^{(k)} > \beta_b^{(k)}\}}, \quad q^{(k)} = \frac{1}{B} \sum_{b=1}^B 1_{\{\alpha_b^{(k)} \leq \beta_b^{(k)}\}} = 1 - p^{(k)}. \quad (\text{A7})$$

The quantities $p^{(k)}$ and $q^{(k)}$ measure the tendency of positive and negative associations, respectively, using the resampling procedure.

Risk map of AIV introduced into poultry farm by wild birds

After matched-pair McNemar analysis, only the bird species with positive association were used to depict a risk map of AIV introduced into poultry farms by wild birds. The risk, defined as an infection probability (R_j), of grid j can be estimated by an *additive-multiplicative* (AM) *risk model* through the decomposition:

$$\hat{R}_j = \text{Pr}(\text{appearance of birds species})^*$$

$$\text{Pr}(\text{introduction of AIV to poultry in grid j} | \text{appearance of bird species})^*$$

$$\text{Pr}\{\text{proportion of poultry farms in area in grid j}\}^*$$

$\text{Pr}\{\text{a poultry farm infected by HPAIV}\}$ (I) The first two terms are estimated, joined by $\frac{\sum_k S_k I_{jk}}{K \times B}$, where the quantities $\{S_k\}$ are the numbers of positively significant association (for species k) in the “B” bootstrapped re-samplings; obviously, $\frac{S_k}{B}$ offers a bootstrap estimate for the “gravity level” of significance, and $\{I_{jk}\}$ are the propensity scores estimated for species k. Let A_j be the number of outbreak poultry farms, D_j be the total number of poultry farms and F_j denotes the total area (in km²) of poultry farms potentially to be infected in grid j. Therefore, the

probability of wild birds introducing AIV into poultry farms in grid j is estimated through the additive model as:

$$\hat{R}_j = \frac{\sum_k S_{kIjk}}{K \times B} \times \frac{A_j}{D_j} \times \frac{F_j}{9 \text{ km}^2}$$

This $(A_j / D_j) \times (F_j / 9 \text{ km}^2)$ can be treated as the proportion (probability) that a randomly selected poultry farm is an infected one in that grid.

References

1. Taiwan Endemic Species Research Institute (TESRI). Taiwan eBird waterfowls hotspots [cited 2020 Aug 5]. https://www.tesri.gov.tw/A6_3/content/32539
2. Lin D, Lin Y, Chao J, Chang A, Pursner S, Lyu A, et al. Taiwan New Year Bird Count 2020 Annual Report. Taiwan Wild Bird Federation, Taiwan Endemic Species Research Institute, Taiwan. 2020.
3. Sullivana BL, Aycrigg JL, Barry JH, Bonney RE, Bruns N, Cooper CB, et al. The eBird enterprise: An integrated approach to development and application of citizen science. *Biol Conserv.* 2014;169:31–40. <https://doi.org/10.1016/j.biocon.2013.11.003>
4. Zou H, Hastie T. Regularization and variable selection via the elastic net. *J R Stat Soc B.* 2005;67:301–20. <https://doi.org/10.1111/j.1467-9868.2005.00503.x>
5. Tibshirani R. Regression shrinkage and selection via the lasso. *J R Stat Soc B.* 1996;58:267–88. <https://doi.org/10.1111/j.2517-6161.1996.tb02080.x>

6. Anselin L. Spatial econometrics: methods and models. Dordrecht: Kluwer Academic Publishers; 1988.
7. Greene W. Accounting for excess zeros and sample selection in Poisson and negative binomial regression models [cited 2022 Nov 22]. NYU Working Paper No EC-94-10. 1994.
https://papers.ssrn.com/sol3/papers.cfm?abstract_id=1293115
8. Rosenbaum PR, Rubin DB. The central role of the propensity score in observational studies for causal effects. *Biometrika*. 1983;70:41–55. <https://doi.org/10.1093/biomet/70.1.41>
9. Efron B. Bootstrap Methods: Another Look at the Jackknife. *Ann Stat*. 1979;7:1–26.
<https://doi.org/10.1214/aos/1176344552>